JOURNAL OF CHEMICAL INFORMATION AND MODELING

Article

pubs.acs.org/jcim

Development and Evaluation of an Integrated Virtual Screening Strategy by Combining Molecular Docking and Pharmacophore Searching Based on Multiple Protein Structures

Sheng Tian,[†,§] Huiyong Sun,[†,§] Youyong Li,[†] Peichen Pan,[†] Dan Li,[‡] and Tingjun Hou*[,†,‡]

[†]Institute of Functional Nano & Soft Materials (FUNSOM) and Jiangsu Key Laboratory for Carbon-Based Functional Materials & Devices, Soochow University, Suzhou, Jiangsu 215123, China

[‡]College of Pharmaceutical Sciences, Zhejiang University, Hangzhou, Zhejiang 310058, China

Supporting Information

ABSTRACT: In this study, we developed and evaluated a novel parallel virtual screening strategy by integrating molecular docking and complex-based pharmacophore searching based on multiple protein structures. First, the capacity of molecular docking or pharmacophore searching based on any single structure from nine crystallographic structures of Rho kinase 1 (ROCK1) to distinguish the known ROCK1 inhibitors from noninhibitors was evaluated systematically. Then, the naïve Bayesian classification or recursive partitioning technique was employed to integrate the predictions from molecular docking and complex-based pharmacophore searching based on multiple crystallographic structures of ROCK1, and the integrated protocol yields much better performance than molecular docking or complex-based pharmacophore searching based on any single ROCK1 structure. Finally, the well-validated integrated virtual screening protocol was applied to identify potential inhibitors of ROCK1 from traditional chinese medicine (TCM). The obtained potential active compounds from TCM are structurally novel and diverse compared with the known inhibitors of ROCK1, and they may afford valuable clues for the development of potent ROCK1 inhibitors.

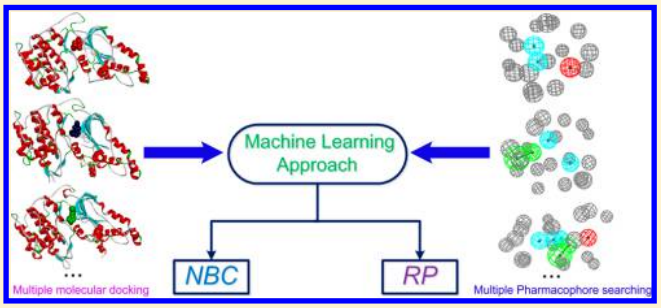

INTRODUCTION

Despite the advances in technology and better understanding of biological systems, drug discovery is still an expensive, inefficient and lengthy process.[1] In a drug discovery campaign, the experimental approach of high-throughput screening (HTS) has been widely used to screen large chemical libraries for finding lead compounds. However, HTS requires large compound libraries purchased from vendors or a large number of compounds synthesized prior to assay, and not every assay can be automated for HTS. As a complementary approach to experimental HTS,[2,3] virtual screening (VS) has gained more and more attention. By taking advantage of the high-performance computers, VS based on a variety of computational techniques or theoretical models can evaluate chemical structures in large libraries rapidly.[4,5]

The VS approaches are historically classified into two categories: ligand-based and structure-based. When the structural information of a drug target is unknown, ligand-based drug design (LBDD) approaches, including drug-likeness filters,[6] quantitative structure−activity relationship (QSAR) models, ligand-based pharmacophore searching, etc., derived from a set of known active ligands, are employed to scan a compound library. When the crystal structure of a drug target is available, the structure-based drug design (SBDD) approaches, such as molecular docking and protein-based pharmacophore searching, can be utilized to find those compounds that are most likely to bind the drug target through evaluating the binding complementary between the target and each compound.

The individual VS method is facing some thorny problems that need to be solved.[7,8] For example, the well-established molecular docking approach needs more accurate scoring functions to predict the protein−ligand binding affinity.[9,10] As reported in previous studies, the dilemma of scoring functions can be partially solved by using consensus scoring schemes.[11−13] Since each VS method has its own shortcomings, it cannot be expected that any of them can consistently perform well under all circumstances. According to the point made by Sheridan and Kearsley, "different methods may select different subsets of actives for the same biological activity and the same method might work better on some activities than others".[14] In order to take advantages of different VS methods, the combined strategies for VS have been proposed in a sequential or parallel manner.[8,15−17] For the sequential VS strategy, the compounds in a screening database are evaluated sequentially by different LBDD or/and SBDD approaches until the number of the final hits for experimental verification is small enough. For the

Received: July 3, 2013
Published: September 7, 2013

   dx.doi.org/10.1021/ci400382r | J. Chem. Inf. Model. 2013, 53, 2743−2756

parallel VS strategy, the applied LBDD or/and SBDD approaches are employed independently and the top hits were retrieved by combining the results given by different approaches. The sequential VS strategy has been widely used in traditional drug design pipeline, but it is sensitive to some inherent limitations, such as the order of the employed approaches.[15] Since the inherent limitations of the sequential VS strategy cannot be easily solved, the parallel VS strategy may be a better choice. The philosophy behind the parallel VS strategy is that the predictions from different VS are supplementary to each other.[15] Therefore, the combination or fusion of the results from multiple LBDD or/and SBDD approaches has been proved to be efficient to improve prediction accuracy.[18] Besides, the parallel combination of different LBDD or/and SBDD approaches can enhance the probability of finding more diverse active compounds for a target of interest.[19]

There are plenty of ways to combine multiple VS approaches in a parallel manner. The simplest but popular way is to combine all top ranked hits given by each individual method for experimental assays or the next step of VS. For example, Chen et al. applied a parallel VS protocol to identify potent lead compounds against phosphodiesterase 4 (PDE4) from the SPECS database. All hits chosen by the searching of ten effective pharmacophore models were retained for molecular docking and bioassays, and finally four promising active compounds were found.[20] In addition, the LBDD or/and SBDD approaches can be combined in different ways by using more complicated data fusion strategies. As a popular data fusing strategy, the consensus scoring methods have been proved to be more effective than a single method to distinguish the active from nonactive compounds for a specified target.[12,13,21−24] However, the consensus scoring by simply adding or averaging the ranks from different methods was found to be quite sensitive to an individual method and therefore affected easily by the underlying shortcomings of this individual method in a parallel VS application.[25] Moreover, machines learning techniques have been employed to integrate the results from multiple VS approaches. For example, Klon et al. observed that the screening enrichment can be improved by a combination of consensus scoring and naive Bayesian categorization based on the predictions from five scoring functions.[26]

In our study, we proposed an efficient and reliable parallel VS strategy by integrating the predictions from molecular docking and complex-based pharmacophore searching by using machine learning approaches. Moreover, as shown in the previous studies, the VS based on a single pharmacophore model might not be efficient to identify active compounds from compound library.[20,27−30] In addition, the previous studies illustrate that the performance of molecular docking is quite sensitive to the protein structures used in calculations.[31−33] The predictions of molecular docking based on multiple structures of a same protein given by experiments or theoretical calculations may complement each other, and then they can be merged to minimize the induce-fit effect of the target.[33−37] Therefore, nine crystallographic structures of Rho kinase 1 (ROCK1) in complex with different inhibitors were used for molecular docking and complex-based pharmacophore generation. For each complex, the capacity of molecular docking or complex-based pharmacophore searching to distinguish the known ROCK1 inhibitors from noninhibitors was evaluated. Then, two machine learning techniques, including naïve Bayesian classification (NBC) and recursive partitioning (RP), were employed to integrate the predictions from molecular docking and complex-based pharmacophore searching based on multiple ROCK1 structures. The integrated classifiers show much better performance than molecular docking or complex-based pharmacophore searching only based on any single protein structure. Finally, the best integrated classifier was utilized to identify the potential ROCK1 inhibitors from traditional chinese medicine (TCM). ROCK is a serine/threonine protein kinase that belongs to RhoGTP-binding protein,[38] and it is involved in a variety of diseases, such as cardiovascular disorders,[39] cancers,[40] nervous system diseases,[41] etc. Until now, only one ROCK inhibitor, fasudil, has been approved in Japan, for preventing cerebral vasospasm after subarachnoid hemorrhage.[42] It is definitely necessary and extremely urgent to identify promising ROCK inhibitors from huge chemical space for treating related diseases.

METHODS AND MATERIALS

Preparation of ROCK1 Complexes and Validation Data Set. The workflow of the integrated VS protocol is illustrated in Figure S1 in the Supporting Information. The crystallographic structures of nine ROCK1−inhibitor complexes were retrieved from the RCSB protein data bank[43] (Table S1 in the Supporting Information). The validation data set with the inhibitors and noninhibitors of ROCK1 was prepared to evaluate the prediction accuracy of molecular docking and complex-based pharmacophore searching. The 350 nonduplicated inhibitors of ROCK1 were obtained from the BindingDB database,[44] and the noninhibitors were randomly chosen from the ChemBridge database by using the *Find Diverse Molecules* protocol in Discovery Studio 3.1;[27] and they had the maximum diversity evaluated by the 2-D similarities (*Tanimoto coefficient*) based on the FCFP_4 fingerprints.[45] The known inhibitors and noninhibitors were compared, and the duplicates were removed from the noninhibitor subset. To mimic the unbalanced nature of inhibitors versus noninhibitors, the ratio of noninhibitors versus inhibitors was set to 20. At last, 350 known inhibitors and 7000 noninhibitors were used for the following analysis.

Validation of Molecular Docking. The crystallographic structures of nine ROCK1 complexes listed in Table S1 in the Supporting Information were employed in our study. Molecular docking calculations were accomplished with *Glide*[46] in Schrodinger 9.0.[43] For each complex, the *Protein Preparation Wizard* in Schrödinger 9.0 was used to remove crystallographic water molecules, add hydrogen atoms, assign partial charges with the OPLS-2005 force field,[47] assign protonated states, and minimize the structure. The minimization was terminated when the average root-mean-square deviation (RMSD) of the non-hydrogen atoms reached a maximum value of 0.3 Å.

The 350 known inhibitors and 7000 noninhibitors in the validation data set were processed using the *LigPrep* module in Schrodinger.[43] For each compound, the ionized states and tautomers were generated by using *Epik* at pH = 7.0. The original chiralities were retained for the inhibitors with known 3D structures. For the noninhibitors without 3D structures, the different combination of chiraties were generated (the maximum number of the stereoisomers for each molecule was set to 32). At last, the validation data set has 350 structures of inhibitors and 12 474 structures of noninhibitors.

By using the *Receptor Grid Generation* component of *Glide*,[46] the bounding box of size 10 Å × 10 Å × 10 Å was defined for

each system and centered on the cocrystallized ligand in the active site. The default settings were used for the grid generation. All structures in the validation data set were docked into the binding site of each protein and scored by the Standard Precision (SP) or Extra Precision (XP) scoring modes. Five thousand poses per ligand were generated during the initial phase of docking, and out of which the best 400 poses were chosen for energy minimization by 100 steps of conjugate gradient minimizations with the dielectric constant of 2.0. The best binding pose for each molecule was saved for the following analysis.

Validation of Protein-Based Pharmacophore Screening. The complex-based pharmacophore models (or interaction patterns) for nine ROCK1 complexes were generated by using the *Receptor−Ligand Pharmacophore Generation (RLPG)* protocol in DS3.1.[27] A set of predefined interaction patterns or pharmacophoric features that include hydrogen bond acceptor/donor (HBA/HBD), hydrophobic (HYD), negative/positive ionizable (PI/NI), and ring aromatic (RA) features of ligands are identified from each receptor−ligand complex and subsequently pruned when not satisfying the protein−ligand interactions using the adjustable topological rules.[48]

For each pharmacophore model, the minimum number of the pharmacophoric features was set to three, and the maximum number was set to the same number of the total features that can match the protein−ligand interactions. Up to 10 pharmacophore models ranked by the selectivity for each complex were generated. The selectivity of each pharmacophore model was measured by a rule-based scoring function based on the genetic function approximation (GFA) technique.[7,49] It must be pointed out that the discrimination capacity which is determined by the ability to distinguish the inhibitors from noninhibitors is more important than the selectivity for the VS based on a pharmacophore model. The ultimate goal of VS is not only to get more positives (active compounds) but also to avoid high rate of false positives (the inactive compounds that are predicted as active ones). By using the *Conformation Generation* protocol in DS3.1,[27] the low-energy conformations of each molecule in the validation data set were generated and the number of the maximum conformations per molecule was set to 100. The discrimination capacity of each pharmacophore model was evaluated.

Integration of the Predictions from Molecular Docking and Pharmacophore Searching by Machine Learning Techniques. Each molecule in the validation data set was docked into the binding site of each protein structure, and also mapped onto the pharmacophore model derived from each ROCK1 complex. Each molecule can be quantitatively assessed by a docking score given by molecular docking and a fit value given by pharmacophore mapping. In total, nine docking scores and nine fit values were generated for each molecule. Those docking scores and fit values were used as the independent variables (X) for generating the integrated models. The value of the response variable Y was 1 for an inhibitor and 0 for a noninhibitor.

Here, naïve Bayesian classification (NBC) and recursive partitioning (RP) were employed to generate the classifiers. The effectiveness of NBC and RP for binary classification has been extensively validated in our previous studies.[50−52] NBC can process large amount of data and learn fast and is tolerant of random noise. It only requires a small amount of training data to estimate the parameters (means and variances of the variables) necessary for classification. Moreover, in the scheme of NBC, the class of a compound can be quantitatively evaluated by the posterior probability. The RP technique mimics the human learning and classification process by splitting a data set into smaller and smaller subsets with a set of hierarchical rules, and at each level, the data have higher purity with regard to a property of interest than the one above. The result of RP is represented by a "decision tree" or "graph" that divides the studied samples into smaller and smaller groups (every group is called a node) according to whether a particular selected predictor is above a chosen threshold or not.[53] Because the RP technique is easily understood, it has been widely used by experimental scientists.

First, the NBC technique was employed to develop classifiers that distinguish the known inhibitors from noninhibitors of ROCK1, and then, the RP technique was employed. In order to evaluate the impact of the maximum tree depth on the performance of a RP model, different RP models were built by changing the tree depth from 4 to 15. Finally, the classification capacities of the classifiers based on NBC and RP were compared under the same condition (same variables, training set and test set). In this study, 5-fold cross-validation was used to evaluate the actual prediction capability for each classifier. All classifiers were developed in DS3.1.[27]

Each classifier was assessed by the following parameters, including true positive (TP), false positive (FP), true negative (TN), and false negative (FN), sensitivity (SE), specificity (SP), global accuracy (GA), and Matthews correlation coefficient (C) as shown in eq 1.

$$C = \frac{\mathrm{TP}\cdot\mathrm{TN} - \mathrm{FN}\cdot\mathrm{FP}}{\sqrt{(\mathrm{TP}+\mathrm{FN})(\mathrm{TP}+\mathrm{FP})(\mathrm{TN}+\mathrm{FN})(\mathrm{TN}+\mathrm{FP})}} \quad (1)$$

Besides, the classification capability was measured by the area under receiver operating characteristic (ROC) curve (AUC) that is a graphical plot to illustrate the performance of a binary classifier by changing its discrimination threshold.

Screening the TCM Compound Database Using the Best Integrated Model. The best Bayesian classifier was then utilized to virtually screen the compounds with molecular weight less than 600 from Traditional Chinese Medicine Compound Database (TCMCD) developed in our group.[51,54,55] Finally, 50 339 TCM compounds were submitted to VS. Each TCM compound was docked into the binding sites of eight ROCK1 structures and mapped onto the pharmacophore models generated from eight ROCK1 complexes. Then, based on the obtained docking scores and fit values, the Bayesian score of each compound was predicted by the best Bayesian classifier. Then, the potential inhibitors of ROCK1 from TCM predicted by the best naïve classifier were assessed by the Lipinski's "rule-of-five"[6] and the REOS (rapid elimination of swill).[4]

RESULTS AND DISCUSSION

Performance of Docking-Based VS. First, as an important measurement of the prediction accuracy and reliability of molecular docking, the "docking power" was evaluated. For each ROCK1 complex, the cocrystallized inhibitor was extracted and redocked into the binding site. The root-mean-squared-deviation (RMSD) between the docked structure and the original conformation of the inhibitor in each complex was calculated. If the RMSD of the docked pose is less than or equal to 2.0 Å from the experimentally

observed conformation, the prediction is regarded to be successful. As shown in Table 1, the Glide docking can successfully recognize the near-native conformations of the cocrystallized inhibitors for most ROCK1 complexes. The only exception is 2V55, and the predicted binding structure by using either SP or XP scoring cannot satisfy the criterion of RMSD ≤ 2.0 Å.

Table 1. Docking Power and Discrimination Power of the Glide Docking for Nine Protein Structures of ROCK1

	P value		RMSD (Å)	
PDB ID	SP	XP	SP	XP
2ESM	8.53×10^{-166}	2.35×10^{-175}	0.52	0.78
2ETR	7.81×10^{-183}	5.10×10^{-152}	0.66	0.24
3D9V	4.14×10^{-143}	9.13×10^{-176}	0.26	1.85
2V55	3.89×10^{-184}	1.84×10^{-189}	2.33	2.43
3NCZ	3.80×10^{-150}	2.18×10^{-166}	0.27	0.17
3NDM	2.30×10^{-120}	1.32×10^{-149}	0.48	0.42
3V8S	4.19×10^{-144}	3.12×10^{-172}	0.53	0.14
3TV7	1.04×10^{-185}	8.80×10^{-224}	1.12	1.47
3TWJ	7.97×10^{-155}	4.83×10^{-179}	4.49	0.59

Then, the "discrimination power" of docking to distinguish the known inhibitors from noninhibitors in the validation data set was examined. The student's *t*-test was employed to evaluate the significance of the difference between the means of the two distributions of the Glide SP or XP scores for the known inhibitor and noninhibitor classes. As shown in Table 1, molecular docking can efficiently distinguish the known inhibitors from noninhibitors for the entire nine complexes, indicated by the quite low *P*-values ($<10^{-20}$). However, the predictions for some structures still show variable discrimination powers. For example, the *P*-value of the SP scoring for 3TV7 is 1.04×10^{-185}, while that for 3NDM is only 2.30×10^{-120}. The distributions of the SP or XP scores with better discrimination power for each complex are depicted in Figure 1. The XP scoring mode is believed to be more accurate than the SP scoring mode, but our results illustrate that the SP scoring does not always give worse performance than the XP scoring. For example, for 2ETR, the *P*-values for the SP and XP scoring modes are 7.81×10^{-183} and 5.10×10^{-152}, respectively (Table 1). Therefore, the comparison between the performance of the SP and XP scoring modes is necessary for a specific target of interest in Glide docking study. In summary, molecular docking with Glide can fulfill the requirement of satisfactory "docking power" (RMSD ≤ 2.0 Å) and "discrimination power" (*P*-value ≤ 10^{-20}) for eight out of nine complexes of ROCK1. Thus, the Glide docking-based VS can be used as a reliable tool to find potential inhibitors of ROCK1.

In order to examine the structural differences of the potential active compounds identified by molecular docking based on

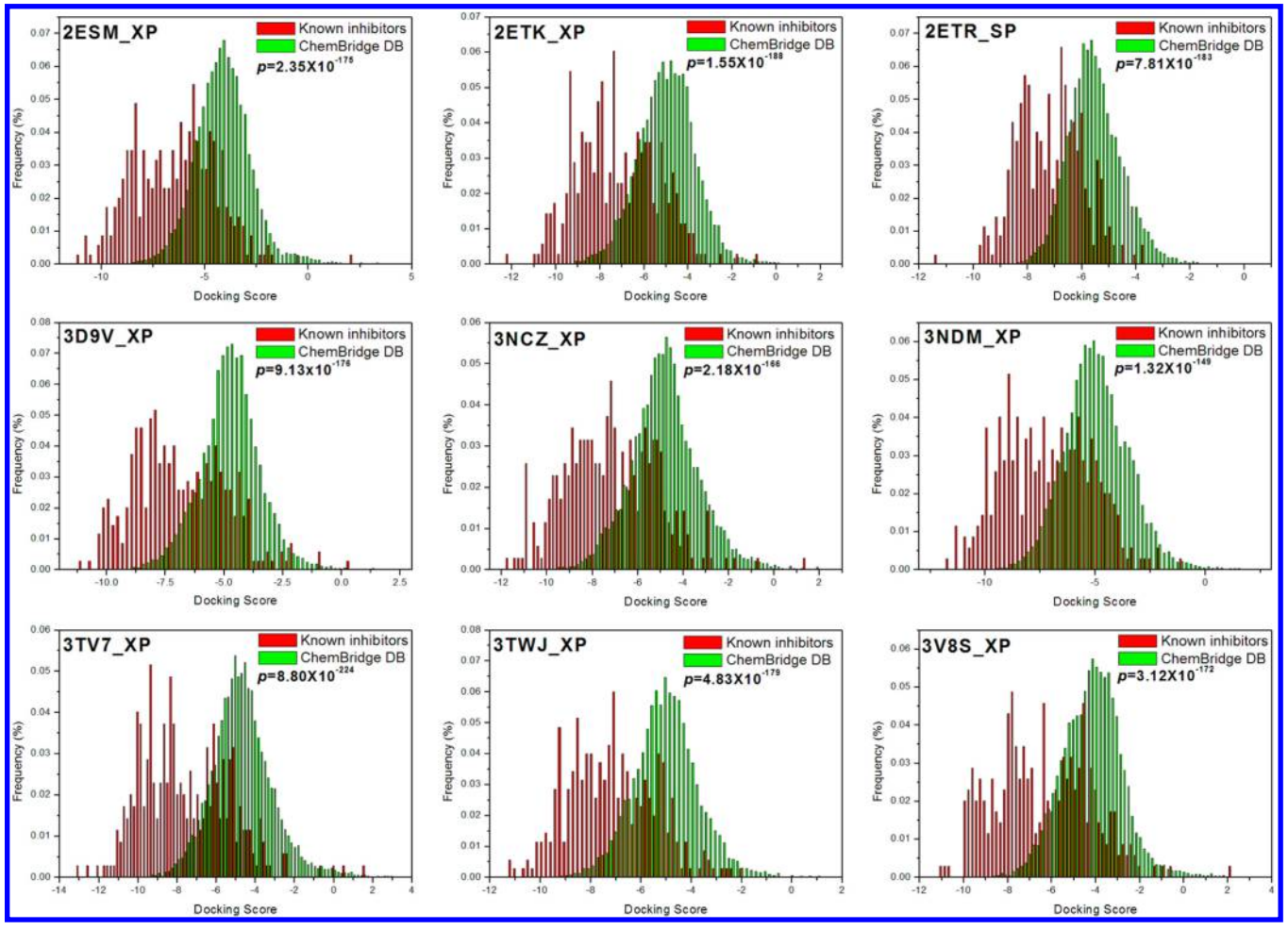

Figure 1. Distributions of the docking scores of the validation data sets for each ROCK1 complex with the best discrimination power.

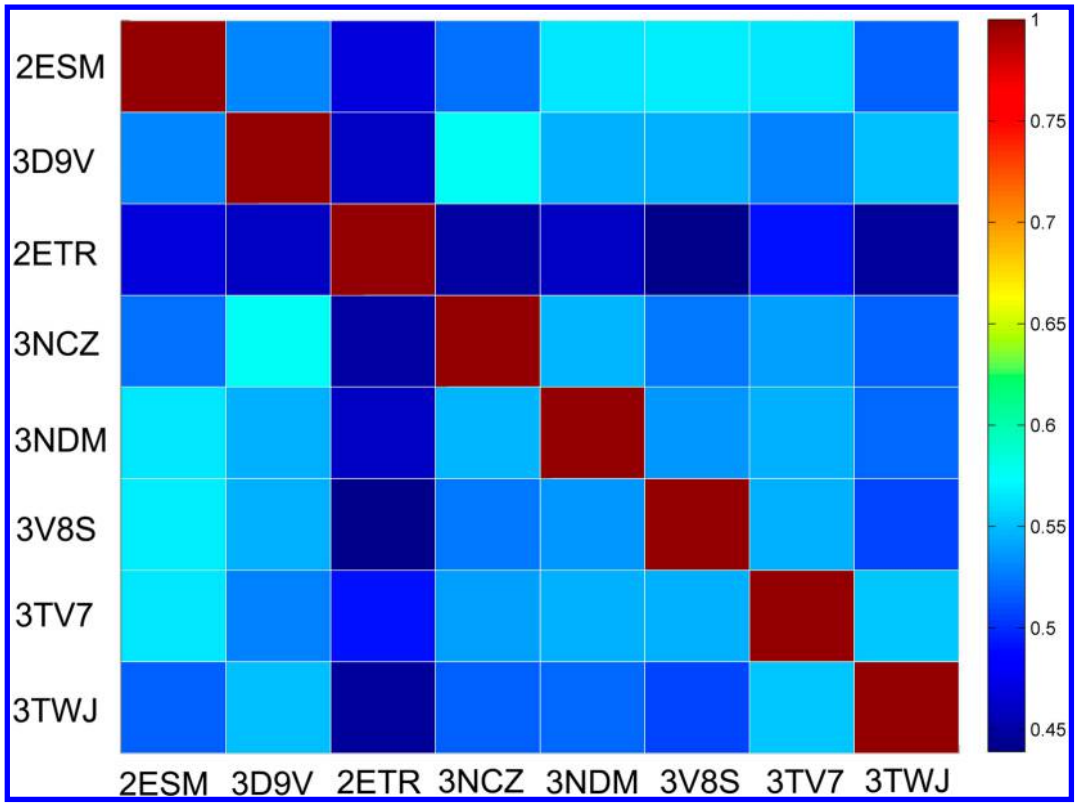

Figure 2. Structural similarities based on the similarity scores of Assemblies for the top 1% molecules from TCM ranked by the docking scores chosen by eight molecular docking studies. The red square and blue square indicate higher and lower structural similarity.

Table 2. Numbers of Total Features and Feature Sets A and B and the Selectivity and Discrimination Capabilities of the Pharmacophore Models Based on Feature Sets A and B

ID	total features	feature set A	selectivity score	AUC	feature set B	selectivity score	AUC
2ESM	AHHP	HHP	−0.2982	0.610	HHP	−0.2982	0.610
2ETR	no pharmacophore can be enumerated with the minimum feature−distance criteria						
3D9V	AHHH	AHHH	0.4772	0.536	AHH	−0.2982	0.548
2V55	AADDDNNNN	AADDDNNNN	14.991	0.501	ADDNNNN	11.692	0.558
3NCZ	AADHHHP	AADHHP	3.0446	0.502	AHHHP	1.4740	0.610
3NDM	ADHHHHP	ADHHHP	3.0446	0.527	ADHHP	1.8263	0.592
3V8S	ADDH	DDH	0.9772	0.631	DDH	0.9772	0.631
3TV7	AADHHHH	AADHHH	3.0446	0.572	AADHH	1.8263	0.609
3TWJ	ADHH	DHH	0.3395	0.662	DHH	0.3395	0.662

different structures of complexes, the similarities of the top 1% molecules from TCM ranked by the docking scores chosen by eight molecular docking studies were compared based on the similarity score of *Assemblies* by using the *Compare libraries* protocol in DS3.1. The statistical results are summarized in the Table S2 in the Supporting Information and depicted in Figure 2. The top 1% hits predicted by molecular docking based on different ROCK1 structures are obviously structurally different, indicated by relatively low similarity scores (Table S2 in the Supporting Information and Figure 2). The highest similarity is less than 0.6. The results demonstrate that the active compounds predicted by molecular docking are dependent on the conformations of the protein structures used for molecular docking. On the basis of the above observations, using multiple available structures of the target of interest for molecular docking is a better choice to find more diverse potential active compounds.

Performance of Pharmacophore-Based VS. All the nine complexes of ROCK1 were used to generate the complex-based pharmacophore models. Eight pharmacophore models were successfully built and no pharmacophore model was generated for the 2ETR complex because the minimum feature distance criterion (<1.0 Å) could not be satisfied.

For each complex, the generated pharmacophore models were ranked by the selective scores detected by the GFA technique. Furthermore, the prediction capacity of each pharmacophore model to distinguish the known inhibitors from noninhibitors was evaluated and ranked by the AUC values. All pharmacophoric features derived from the protein−ligand interactions (total features), the pharmacophoric features of the pharmacophore model with the highest selectivity (feature set A) and those with the highest discrimination power (feature set B) were counted and compared (Table 2). It is expected that a pharmacophore model with more pharmacophoric features would be more selective than that with less pharmacophoric features. According to our results (Table 2), the numbers of feature set A for the most selective pharmacophore models detected by GFA are not always

dx.doi.org/10.1021/ci400382r | J. Chem. Inf. Model. 2013, 53, 2743−2756

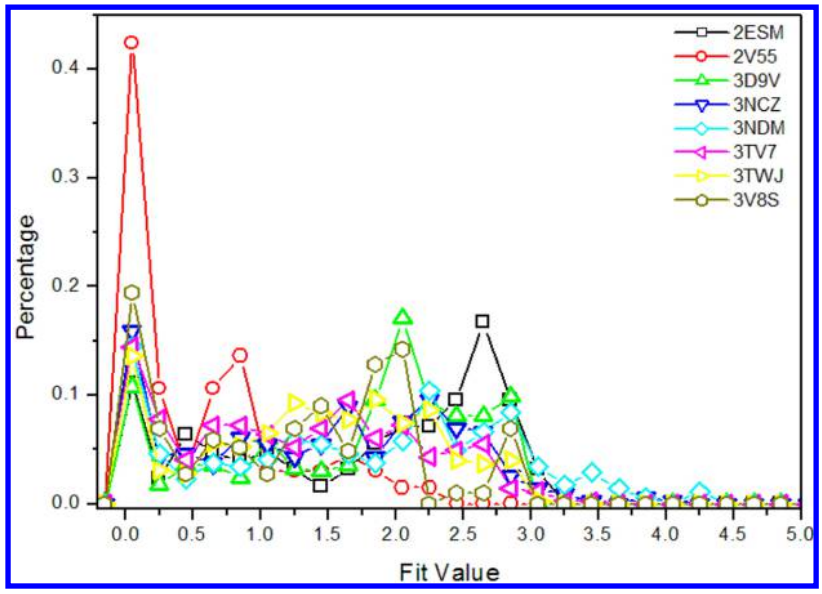

Figure 3. Distributions of the fit values of the retrieved known inhibitors for different pharmacophore models.

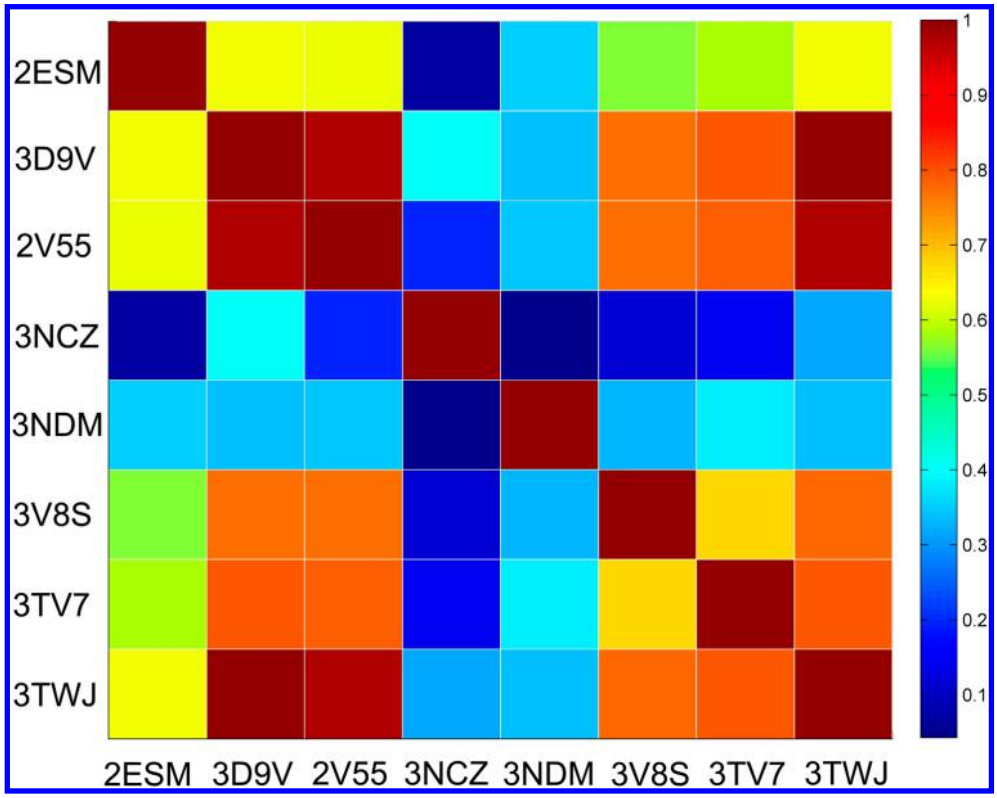

Figure 4. Structural similarities based on the similarity scores of Assemblies for the potential active compounds predicted by different pharmacophore models. The red square and blue square indicate higher and lower structural similarity.

equal to those of total features. Among the eight pharmacophore models, two have the same numbers of feature set A and total features and six have one less number of feature set A than total features. The aim of VS is to find more active molecules while avoid high rate of false positives. The results demonstrate that the pharmacophore models using total features or feature set A with the best selectivity detected by GFA would identify more potential active compounds but simultaneously yield much more false positives. The pharmacophore models using feature set B with the highest discrimination power are more suitable for VS. The eight pharmacophore models with feature set B derived from the eight ROCK1 complexes are depicted in Figure S2 in the Supporting Information.

To our disappointment, as shown in Table 2, the performance of the pharmacophore model with the highest AUC (0.662) would not be good. On the basis of our analysis, the pharmacophoric features derived from different receptor−ligand complexes are quite different. For example, the total features and feature sets A and B of 2ESM and 3NCZ are

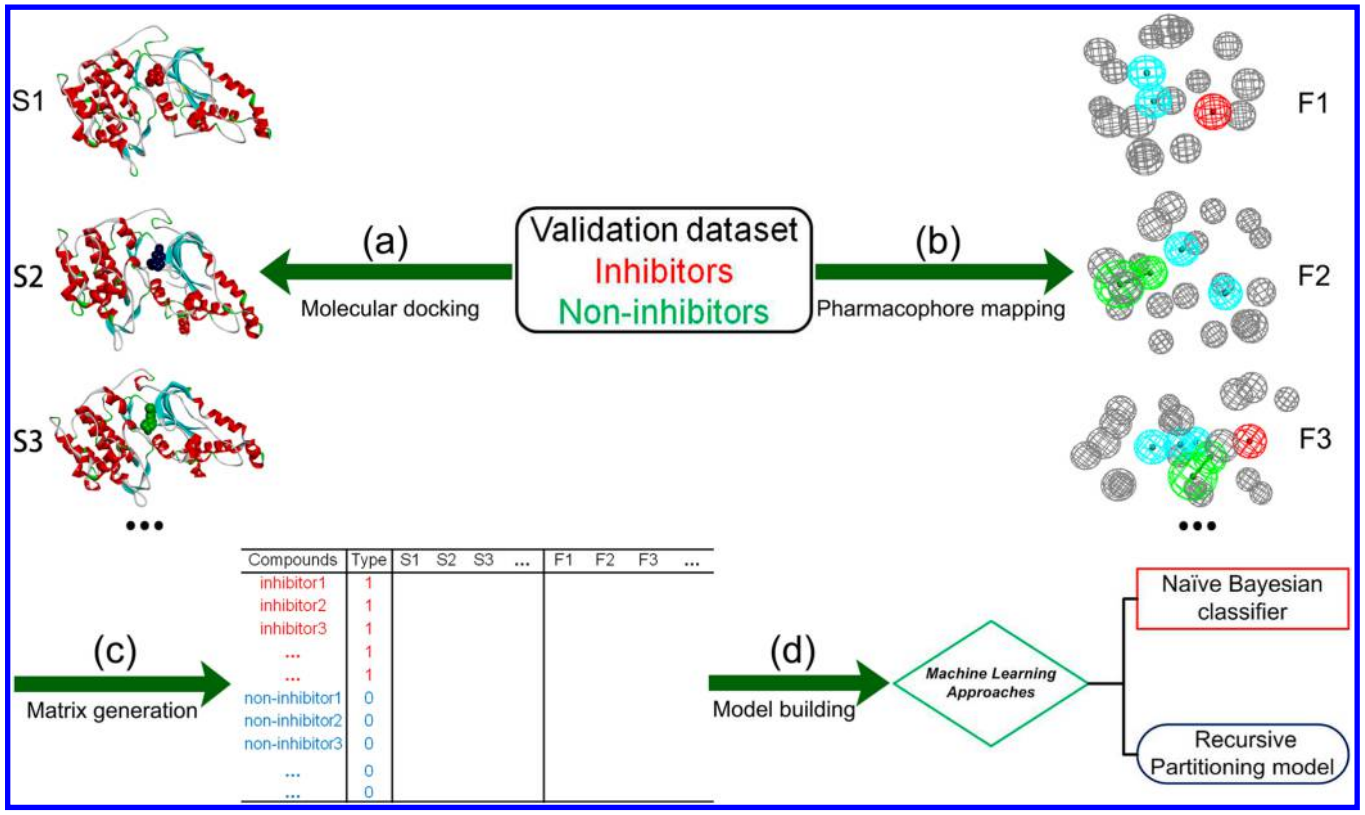

Figure 5. Pipeline of the procedure to build the parallel VS protocol. (a) Dock each molecule in the validation data set into each protein by using the more reliable scoring mode of Glide. (b) Map each molecule in the validation data set onto each pharmacophore model with the most discrimination capacity. (c) Combine the docking scores and fit values for all the compounds in the validation data set to generate the data matrix. (d) Develop the integrated models to discriminate the known inhibitors from noninhibitors by using NBC or RP.

AHHP, HHP, and HHP and AADHHHP, AADHHP, and AHHHP, respectively. Obviously, the binding patterns of the two inhibitors in the binding pockets of 2ESM and 3NCZ are quite different. In order to analyze the performance of different pharmacophore models, all of the known ROCK1 inhibitors were mapped onto eight generated pharmacophore models. The number of known ROCK1 inhibitors that can be mapped onto each pharmacophore model, and the number of the mapped ROCK1 inhibitors with the fit values above 2.0 are listed in Table S3 in the Supporting Information. For the pharmacophore models generated from different complexes, the numbers of the retrieved known inhibitors are different for some systems. Besides, the distributions of the fit values for the retrieved known inhibitors for the pharmacophore models are depicted in Figure 3, and the different distributions suggest that different complex-based pharmacophore models yield different prediction performance. Furthermore, if the fit value above 2.0 is regarded as a good mapping, the numbers of the mapped known inhibitors for different pharmacophore models are quite different. For example, the number of the known inhibitors mapped onto the pharmacophore models generated from 3NDM and 2V55 complexes with the fit values above 2.0 are 160 and 2, respectively, which further proves that the pharmacophore models generated from different ROCK1 complexes are different in terms of prediction capacity for known inhibitors.

Finally, we compared the prediction results of the pharmacophore models derived from different complexes by screening the compounds in TCMCD. As can be seen from Table S4 in the Supporting Information, the numbers of the potential active compounds with the fit values above 2.0 for individual pharmacophore models are quite different. For example, there are only 226 potential active compounds predicted by the pharmacophore model derived from 3NDM. In contrast, the four pharmacophore models derived from the complexes 3D9V, 2V55, 3NCZ, and 3TWJ can find more than 5000 potential active compounds, and the three pharmacophore models derived from the complexes 2ESM, 3V8S, and 3TV7 can find potential active compounds from TCMCD between 1000 and 2000. In addition, the structural similarities of the potential active compounds predicted by different pharmacophore models are compared based on similarity score of *Assemblies* by using the *Compare libraries* protocol in DS3.1. According to the statistical results summarized in Table S5 in the Supporting Information and plotted in Figure 4, we observe that 15 in total 28 protein pairs have the structural similarities less than 0.6, demonstrating that the predicted active compounds by different pharmacophore models are quite different. In light of observations above, we conclude that different pharmacophore models can yield complementary predictions.

Naïve Bayesian Classifier Based on the Multidocking Scores and Multifit Values. As shown in the above two sections, molecular docking shows satisfactory "docking power" and "discrimination power". Eight out of nine ROCK1 complexes can satisfy the requirements of RMSD $\leq$ 2.0 Å and *P*-value $\leq 10^{-20}$ by using either Glide SP or XP scoring mode (Table 1 and Figure 1). Moreover, indicated by the low AUC value (AUC < 0.7), the pharmacophore models with the best discrimination powers did not show satisfactory

dx.doi.org/10.1021/ci400382r | J. Chem. Inf. Model. 2013, 53, 2743−2756

Table 3. Performances of Naïve Bayesian Classifiers Using Docking Scores and Fit Values As Molecular Descriptors

descriptors	TP	FN	FP	TN	SE	SP	GA	C	AUC
2ESM_S	201	149	1110	11363	0.574	0.911	0.902	0.261	0.752
2ETR_S	93	257	38	12435	0.266	0.997	0.977	0.426	0.784
3D9V_S	230	120	2013	10460	0.657	0.839	0.834	0.213	0.763
3NCZ_S	235	115	2104	10369	0.671	0.831	0.827	0.212	0.783
3NDM_S	218	132	1895	10578	0.623	0.848	0.842	0.207	0.764
3V8S_S	210	140	1474	11002	0.600	0.882	0.874	0.232	0.753
3TV7_S	193	157	348	12125	0.551	0.972	0.961	0.424	0.813
3TWJ_S	222	128	1206	11267	0.634	0.903	0.896	0.278	0.826
2ESM_F	126	224	1062	11411	0.360	0.915	0.900	0.154	0.648
3D9V_F	334	16	6479	5994	0.954	0.481	0.493	0.142	0.714
2V55_F	66	284	592	11881	0.189	0.953	0.932	0.104	0.563
3NCZ_F	340	10	6495	5978	0.971	0.479	0.493	0.147	0.778
3NDM_F	345	5	6630	5843	0.986	0.468	0.483	0.149	0.763
3V8S_F	288	62	3616	8857	0.823	0.710	0.713	0.189	0.776
3TV7_F	326	24	5681	6792	0.931	0.545	0.555	0.155	0.771
3TWJ_F	323	27	3980	8493	0.923	0.681	0.688	0.208	0.795
combined docking score[a]	250	100	1468	11005	0.714	0.882	0.878	0.285	0.874
combined fit value[b]	322	28	3893	8580	0.920	0.688	0.694	0.211	0.879
combined docking score + fit value[c]	289	61	1563	10910	0.826	0.875	0.873	0.325	0.938

[a]Combine all of the docking sores as independent molecular descriptors. [b]Combine all of the fit values as independent molecular descriptors. [c]Combine all of the docking scores and fit values as independent molecular descriptors.

predictions. Meanwhile, it was detected that the pharmacophoric features in different pharmacophore models (Table 2) were quite different. Then, a question would be raised: could the integration of molecular docking and pharmacophore searching based on multiple structures improve the predictions?

All the docking scores and fit values of the compounds in the validation data set for each complex were used to generate the data matrix for model building. The docking scores of the validation data set for 2V55 were excluded because the docking power for 2V55 was not satisfied (RMSD > 2.0 Å). Moreover, no pharmacophore model was generated for 2ETR. Finally, eight sets of docking scores and eight sets of fit values were used as the independent variables to build the classification models to distinguish the known inhibitors from noninhibitors of ROCK1. The flowchart of the model generation process is depicted in Figure 5. It should be noted that some molecules in the validation data set can be neither docked into the binding site of a protein nor mapped onto a pharmacophore model, so the docking scores or fit values of some compounds in the validation data set are missing. Thus, the penalty values were artificially assigned to those compounds with missing docking scores or fit values. Because the maximum docking score and the minimum fit value are approximately 10 and 0, respectively, an initial penalty docking score (PDS) of 20 and an initial penalty fit value (PFV) of −10 were assigned.

First, the Bayesian classifiers were built based on the docking scores and fit values. As seen in Table 3 and Figure 6, most Bayesian classifiers based on a single column of docking scores or fit values give acceptable predictions, indicated by relatively high AUC values (AUC > 0.7). An interesting finding is most Bayesian classifiers based on the fit values derived from a single pharmacophore model have acceptable prediction power (AUC > 0.7). Obviously, the addition of PFV is beneficial for obtaining better predictions.

Then, the other three Bayesian classifiers with the combined docking scores, the combined fit values, and the combination of both docking scores and fit values were built up (Table 3 and Figure 6). The 5-fold cross-validated Matthews correlation coefficients and AUC values for these three Bayesian classifiers are 0.285, 0.211, and 0.325 and 0.874, 0.879, and 0.938, respectively. Apparently, compared with the Bayesian classifiers based on any single column of docking scores or fit values, the classifiers based on the docking scores and/or fit values derived from multiple protein structures perform much better. The best Bayesian classifier based on all the docking scores and fit values achieves a sensitivity of 0.826, a specificity of 0.875, and a global accuracy of 0.873.

As discussed above, some compounds in the validation data set cannot be docked into the binding sites or mapped onto the pharmacophore models, and therefore, two penalty terms, PDS of 20 and PFV of −10, were initially employed for those missing compounds. In order to evaluate the influence of PDS and PFV, multiple Bayesian classifiers were established by changing PDS from 20 to 60 and PFV from −50 to −10. As shown in Table S6 in the Supporting Information, when PFV was set to −10, the prediction power (AUC = 0.933−0.942) of the Bayesian classifiers changes slightly with the change of PDS. Similar phenomenon (AUC = 0.935−0.938) was also observed when PDS was set to 20 and PFV was changed. Our observations illustrate that the variations of the penalty terms do not have significant impact on the prediction accuracies of the Bayesian classifiers. Besides, we can find that when PDS was set to 60 and PFV to −10 the Bayesian classifier achieves the best prediction accuracy (AUC = 0.942). Compared with the other classifiers, the best Bayesian classifier has more balanced prediction capacity. For example, the sensitivity, specificity and global accuracy of the best Bayesian classifier are 0.857, 0.858, and 0.858, respectively, but those of the classifier with PDS of 50 and PFV of −10 are 0.926, 0.790, and 0.793, respectively. According to this observation, the Bayesian classifier with PDS of 60 and PFV of −10 may be more reliable and practical for VS.

Influence of the Ratio of Training Set versus Test Set on Naïve Bayesian Classifiers. In Table 3, the statistical results were obtained from the 5-fold cross-validations. In order to give a more rigorous evaluation of the actual prediction

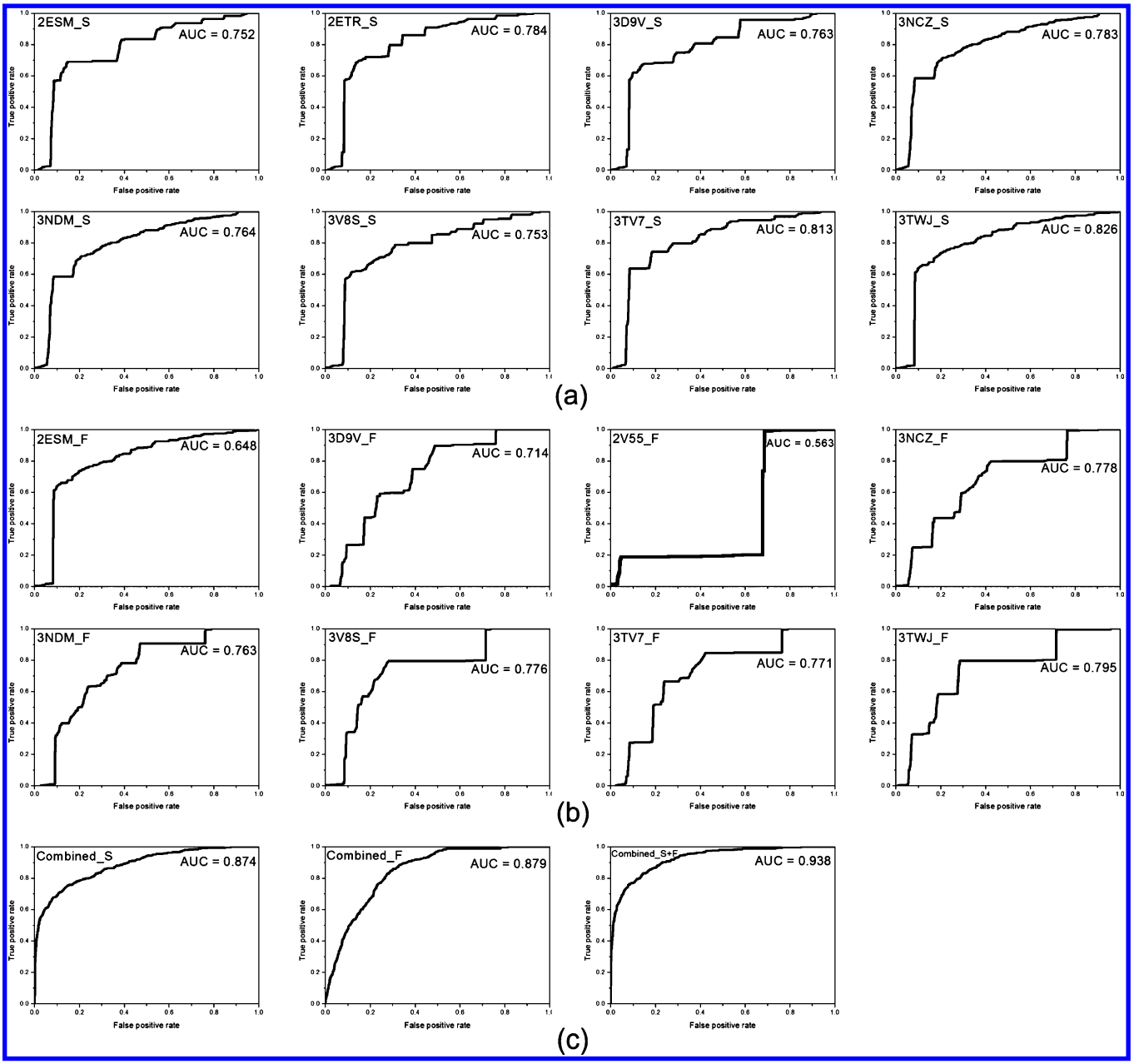

Figure 6. ROC curves of the naïve Bayesian classifiers based on (a) the docking score for each complex, (b) fit value for each complex, and (c) combination of the docking scores and fit values.

accuracy of the Bayesian classifiers, the whole data set was split into a training set and an external test set. The ratio of the training set to test set changes from 9:1 to 1:9. For example, when the ratio was set to 9:1, 90% of the known inhibitors and noninhibitors were randomly selected to form the training set and the remaining compounds were served as the test set. At each ratio, the training and testing were run for 10 times. The performances of the Bayesian classifiers based on different training and test sets are shown in Table S7 in the Supporting Information and plotted in Figure 7. When the ratio changes from 9:1 to 1:9, the prediction accuracy for the training set decreases slightly but that for the test set is almost the same. This implies that even only a small portion of the known inhibitors and noninhibitors were used for training the Bayesian classifier, the obtained classifier can give reliable predictions for the remaining compounds in the test set. The ROC curve of the naïve Bayesian classifier with the ratio of 1:9 based on all of the docking scores and fit values is shown in Figure 8. Apparently, the Bayesian classifiers we built are quite reliable and not overfitting.

Performance of the RP Classifiers. Compared with the Bayesian classifiers, the RP classifiers, also termed as decision trees, can give more understandable classification models defined as a series of hierarchical rules. Therefore, RP was employed to establish decision trees to distinguish the known inhibitors from noninhibitors of ROCK1 based on all the docking scores and fit values derived from multiple protein structures. The prediction accuracy of each RP model was evaluated and compared with that of the naïve Bayesian classifier. During building the RP models, the depth of decision tree, an important parameter to control the complexity of a RP model, was calibrated carefully according to the prediction for

dx.doi.org/10.1021/ci400382r | J. Chem. Inf. Model. 2013, 53, 2743−2756

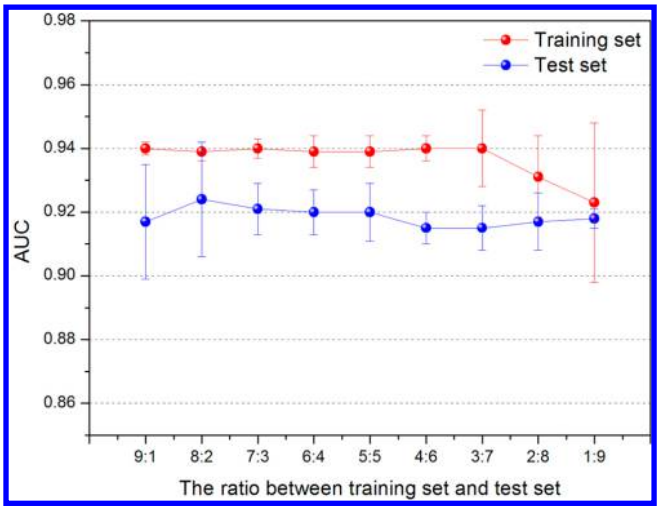

Figure 7. Performances of the naïve Bayesian classifiers by using different ratio of training set versus test set based on the combination of all of the docking scores and fit values.

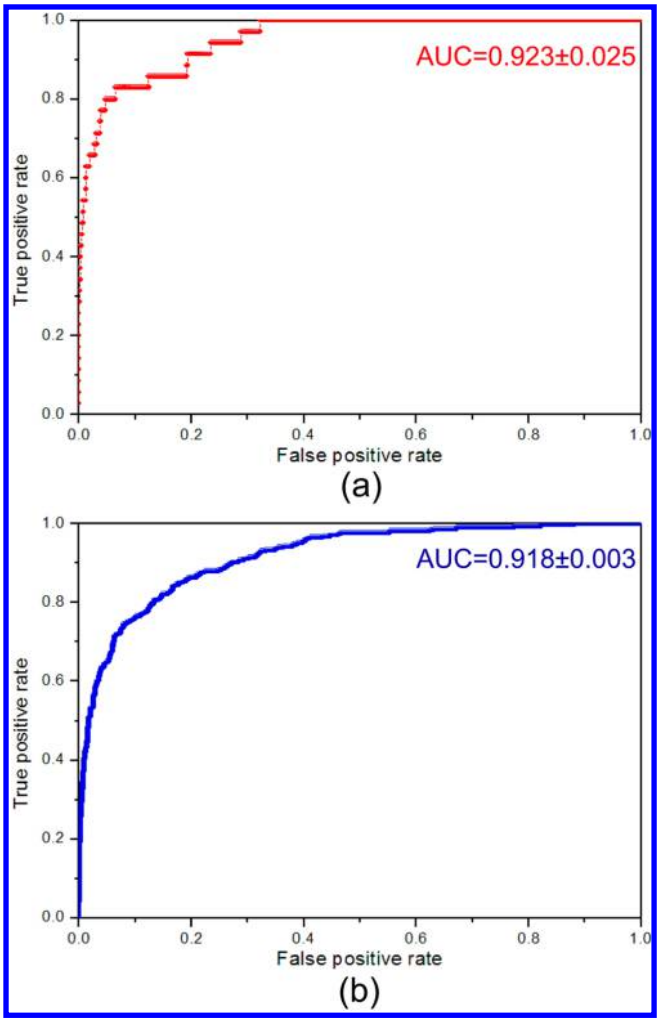

Figure 8. ROC curves of the naïve Bayesian classifiers with the ratio of 1:9 for training set to test set based on the combination of all of the docking scores and fit values.

the test set. Various RP models were built by changing the tree depth from 4 to 15 with the ratio of 9:1. As shown in Tables S8 and S9 in the Supporting Information, the prediction accuracies of the RP models are acceptable according to the 5-fold cross-validated Matthews correlation coefficients. The decision tree with the tree depth of 4 is depicted in Figure 9 as an example. For the test set (Table S9 in the Supporting Information), the *C* value increases to 0.399 at the tree depth of 7 and then decreases slightly. According to this observation, the best RP model was trained when the tree depth was set to 7. The sensitivity, specificity, global accuracy, and *C* value of the best RP model are 0.914, 0.897, 0.897, and 0.399, respectively. On the basis of the same training and test sets, the performance of the best RP model is almost as good as that of the best Bayesian classifier.

Identification of Potential Inhibitors of ROCK1 from TCM. According to the predictions for the test set, the best naïve Bayesian classifiers is slightly better than the best RP classifier. The best Bayesian classifier was then utilized to virtually screen the compounds with molecular weight less than 600 from TCM. On the basis of the obtained docking scores and fit values, the Bayesian score of each compound was calculated by the best Bayesian classifier (Figure 6c). The distributions of the Bayesian scores for the known inhibitors, noninhibitors, and compounds from TCM are shown in Figure 10. Although the optimal threshold of the Bayesian score for distinguishing the inhibitors from noninhibitors given by the Bayesian classifier is 2.075, the distributions of the Bayesian scores for the known inhibitors and noninhibitors overlap strongly between −10 and 10. However, we need to emphasize that due to the unbalanced nature of the data set, the Bayesian classifier will generate so many false positives if the threshold of 2.075 is used. Obviously, a more stringent threshold is necessary to control the number of false positives. By checking the true positive rate and false positive rate at different thresholds (Figure 6c), a more stringent criterion was determined. When the threshold was set to 16.954, the false positive rate is only 0.168% and the true positive rate increases to 30%. That is, when 105 known inhibitors were successfully predicted as true positives, only 20 noninhibitors would be predicted as false positives. When the stringent threshold of the Bayesian score was employed, 277 molecules from TCM were predicted as potential inhibitors of ROCK1. Then, those potential inhibitors were evaluated by Lipinski's rule-of-five,[6] and the candidates that violate more than one rule of rule-of-five were discarded. The remaining compounds were further assessed by the REOS rules to remove the candidates with reactive, toxic, and otherwise undesirable moieties.[4] By employing the hierarchical filters, only 53 potential inhibitors of ROCK1 were obtained from TCM.

The receptor−ligand interactions between the predicted inhibitor with the highest Bayesian score (1-*O*-*β*-D-glucopyranosyl-aloe-emodinand) and eight ROCK1 structures are shown in Figure 11. Then, the structural similarities between the predicted inhibitors from TCM and the known inhibitors of ROCK1 were compared using the Compare Libraries protocol in DS3.1.[27] Three comparison methods based on Assemblies, Bayesian Model, and Global Fingerprint were employed. The Assemblies method calculates the similarity of two libraries evaluated by the 2D similarities (Tanimoto coefficient) based on the unique occurrences of *MurckoAssemblies*, which are contiguous ring systems plus chains that link two or more rings.[56] For the Bayesian model method, two Bayesian classification models for two libraries were first created and then a Bayesian distance based on the two libraries was calculated. The longer the distance is, the more dissimilar the

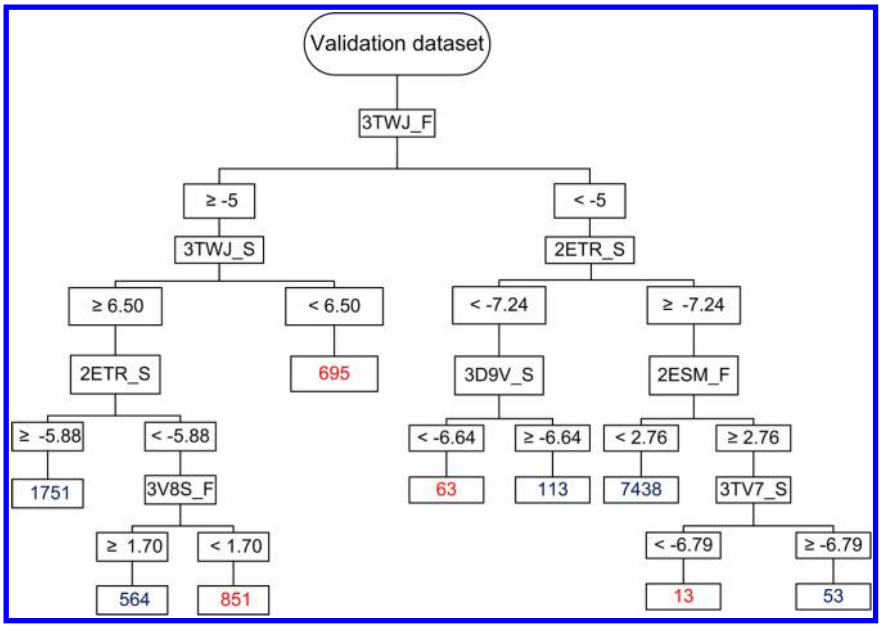

Figure 9. Decision tree of the RP model at the tree depth of 4 with the ratio of 9:1 for training set to test set.

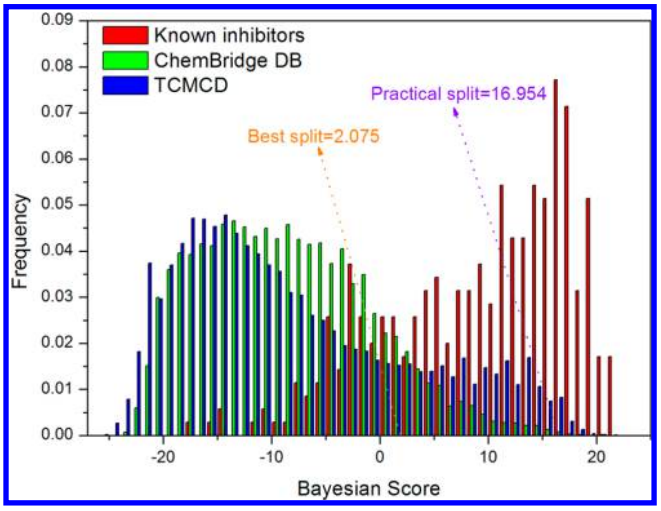

Figure 10. Distributions of the Bayesian scores of known inhibitors, noninhibitors, and compounds from TCM predicted by the most reliable Bayesian classifier.

compared libraries are. The Global Fingerprint method computes the similarity of two libraries evaluated by the Tanimoto distance of the global fingerprints of all molecules from the two libraries based on the ECFP_6 fingerprints. The statistical results show that the predicted inhibitors from TCM were quite structurally different from the known ROCK1 inhibitors. For example, the number of the common MurckoAssemblies between the predicted inhibitors and known inhibitors was only 8, and the numbers of MurckoAssemblies only in the predicted inhibitors and known inhibitors were 37 and 189, respectively. The similarity score of MurckoAssemblies between the two data sets was 0.0342. The Bayesian distance between the two data sets was 187.94. The distributions of the Bayesian scores for the predicted inhibitors and known inhibitors based on the Bayesian classifiers using the known inhibitors and predicted inhibitors were shown in Figure S3 in the Supporting Information. Besides, the similarity score based on ECFP_6 between the two libraries is only 0.0313. Our results suggested that the potential inhibitors predicted from TCM are quite novel. Ten most dissimilar inhibitors and ten most similar inhibitors predicted from TCM to the known ROCK1 inhibitors are shown in Figures 12a and b, respectively.

Finally, the structural diversity of the predicted inhibitors from TCM was also examined. All the 53 predicted inhibitors were classified into 10 clusters based on the similarity of the FCFP_6 fingerprints by using the *cluster ligands* protocol in DS3.1.[27] Ten molecules with the highest Bayesian scores chosen from 10 clusters are shown in Figure 13. On the basis of these observations, the potential inhibitors predicted from TCM are quite novel and have more structural diversity. We believed that the potential inhibitors from TCM may be served as novel leads against ROCK1.

CONCLUSION

In the present study, we have designed and evaluated a parallel VS protocol by integrating the prediction results from molecular docking and complex-based pharmacophore searching based on multiple protein structures of ROCK1. To combine the complementary results from molecular docking and pharmacophore searching based on multiple protein structures, naïve Bayesian classification or recursive partitioning was employed to build the integrated classifiers. It is encouraging to find that the integrated classifiers illustrate much better performance than molecular docking or complex-based pharmacophore searching based on any single ROCK1 structure. Then, the most reliable classifier was utilized to identify potential inhibitors of ROCK1 from TCM. The predicted inhibitors are quite novel compared with the known inhibitors, and they can be served as the starting points for the development of novel ROCK1 inhibitors. The new parallel VS strategy developed here is quite reliable and can be used as a powerful tool in VS for the targets of interest.

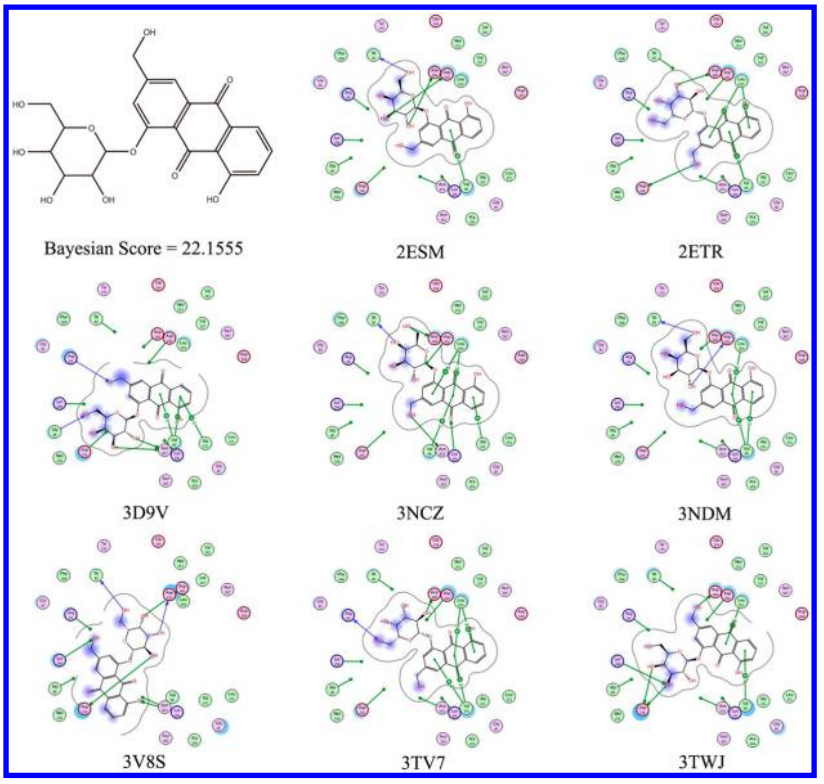

Figure 11. Receptor−ligand interaction between the most promising active compound, 1-*O*-*β*-D-glucopyranosyl-aloe-emodin, and eight proteins of ROCK1.

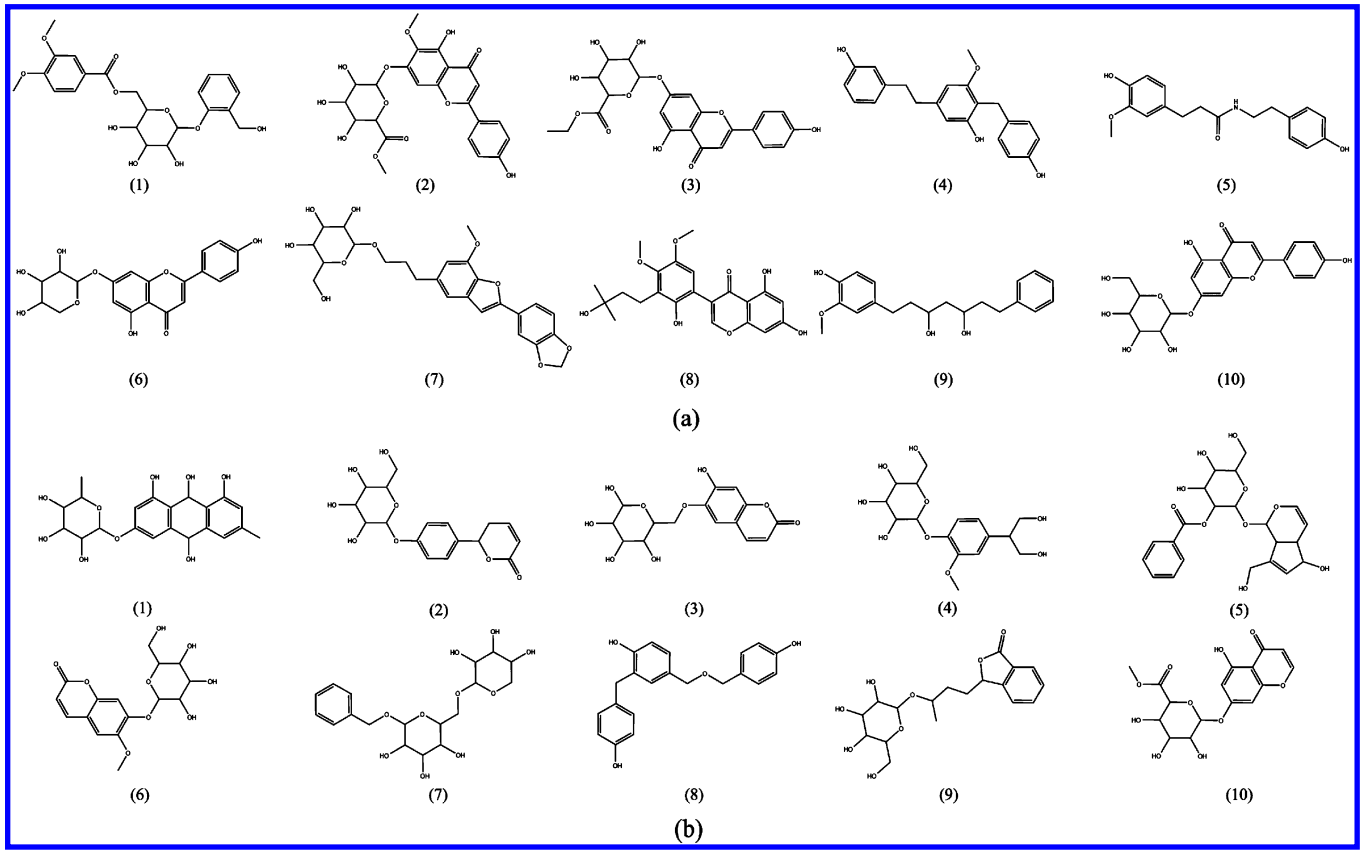

Figure 12. (a) Ten most similar predicted compounds from TCM to the known inhibitors based on the ECFP_6 fingerprints. (b) Ten most dissimilar predicted compounds of TCM to the known inhibitors based on the ECFP_6 fingerprints.

dx.doi.org/10.1021/ci400382r | *J. Chem. Inf. Model.* 2013, 53, 2743−2756

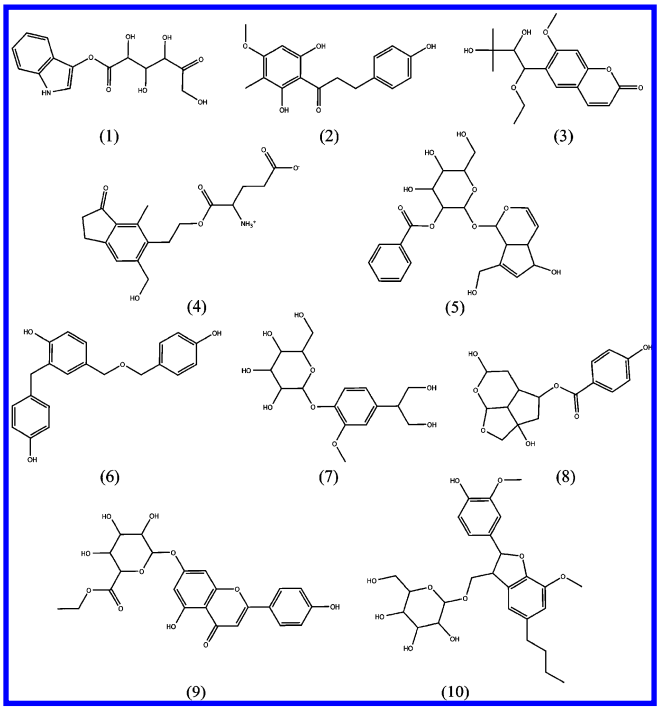

Figure 13. Ten most diverse predicted active compounds from TCM based on the FCFP_6 fingerprints.

■ ASSOCIATED CONTENT

Supporting Information

Table S1: PDB entries, ligand names and resolutions of nine complexes of ROCK1. Table S2: Structural similarity based on the similarity scores of Assemblies for the top 1% compounds from TCM predicted by molecular docking based on different protein structures. Table S3: Numbers of the retrieved known inhibitors predicted by the pharmacophore models derived from the different complexes of ROCK1. Table S4: Number of the potential inhibitors from TCM predicted by the pharmacophore models derived from the different complexes of ROCK1. Table S5: Structural similarity based on the similarity scores of Assemblies for the potential active compounds predicted by the pharmacophore models. Table S6: Influences of the penalty docking score (PDS) and penalty fit value (PFV) on the performance of the naïve Bayesian classifiers. Table S7: Performance of the naïve Bayesian classifiers based on different ratio of training set versus test set. Table S8: Performances of the RP models by changing the tree depth. Table S9: Performances of the RP models for the test set by changing the tree depth. Figure S1: Workflow of the parallel protocol to find potential inhibitors of ROCK1 from TCM. Figure S2: Eight pharmacophore models with the most distinguishing capacity derived from the eight ROCK1 complexes. Figure S3: Distributions of the Bayesian scores for the known inhibitors of ROCK1 and the potential inhibitors of ROCK1 predicted by (a) the Bayesian model built based on the known inhibitors and (b) the Bayesian model built based on the 53 predicted active compounds from TCM. This material is available free of charge via the Internet at http://pubs.acs.org.

■ AUTHOR INFORMATION

Corresponding Author

*E-mail: tingjunhou@hotmail.com or tingjunhou@zju.edu.cn. Phone: +86-512-65882039.

Notes

The authors declare no competing financial interest.

[§]S.T. and H.S. are cofirst authors.

■ ACKNOWLEDGMENTS

This study was supported by the National Science Foundation of China (21173156), the National Basic Research Program of China (973 program, 2012CB932600), and the Priority Academic Program Development of Jiangsu Higher Education Institutions (PAPD)

■ REFERENCES

(1) Anson, B. D.; Ma, J.; He, J.-Q. Identifying Cardiotoxic Compounds. *Genet. Eng. Biotechnol. News* **2009**, *29*, 34−35.

(2) Bajorath, F. Integration of virtual and high-throughput screening. *Nat Rev. Drug Discov.* **2002**, *1*, 882−894.

(3) Klebe, G. Virtual ligand screening: strategies, perspectives and limitations. *Drug Discov. Today* **2006**, *11*, 580−594.

(4) Walters, W. P.; Stahl, M. T.; Murcko, M. A. Virtual screening - an overview. *Drug Discov. Today* **1998**, *3*, 160−178.

(5) Hou, T. J.; Xu, X. J. Recent development and application of virtual screening in drug discovery: An overview. *Curr. Pharm. Des.* **2004**, *10*, 1011−1033.

(6) Lipinski, C. A.; Lombardo, F.; Dominy, B. W.; Feeney, P. J. Experimental and computational approaches to estimate solubility and permeability in drug discovery and development settings. *Adv. Drug Delivery Rev.* **1997**, *23*, 3−25.

(7) Meslamani, J.; Li, J.; Sutter, J.; Stevens, A.; Bertrand, H.-O.; Rognan, D. Protein-Ligand-Based Pharmacophores: Generation and Utility Assessment in Computational Ligand Profiling. *J. Chem. Inf. Model.* **2012**, *52*, 943−955.

(8) Drwal, M. N.; Griffith, R. Combination of ligand-and structure-based methods in virtual screening. *Drug Discov. Today: Technol.* **2013**, *10*, e395−e401.

(9) Warren, G. L.; Andrews, C. W.; Capelli, A.-M.; Clarke, B.; LaLonde, J.; Lambert, M. H.; Lindvall, M.; Nevins, N.; Semus, S. F.; Senger, S.; Tedesco, G.; Wall, I. D.; Woolven, J. M.; Peishoff, C. E.; Head, M. S. A critical assessment of docking programs and scoring functions. *J. Med. Chem.* **2006**, *49*, 5912−5931.

(10) Ferrara, P.; Gohlke, H.; Price, D. J.; Klebe, G.; Brooks, C. L. Assessing scoring functions for protein-ligand interactions. *J. Med. Chem.* **2004**, *47*, 3032−3047.

(11) Wang, R. X.; Lu, Y. P.; Wang, S. M. Comparative evaluation of 11 scoring functions for molecular docking. *J. Med. Chem.* **2003**, *46*, 2287−2303.

(12) Houston, D. R.; Walkinshaw, M. D. Consensus Docking: Improving the Reliability of Docking in a Virtual Screening Context. *J. Chem. Inf. Model.* **2013**, *53*, 384−390.

(13) Teramoto, R.; Fukunishi, H. Supervised consensus scoring for docking and virtual screening. *J. Chem. Inf. Model.* **2007**, *47*, 526−534.

(14) Sheridan, R. P.; Kearsley, S. K. Why do we need so many chemical similarity search methods? *Drug Discov. Today* **2002**, *7*, 903−911.

(15) Tanrikulu, Y.; Kruger, B.; Proschak, E. The holistic integration of virtual screening in drug discovery. *Drug Discov. Today* **2013**, *18*, 358−64.

(16) Sperandio, O.; Miteva, M. A.; Villoutreix, B. O. Combining ligand- and structure-based methods in drug design projects. *Curr. Comput.-Aided Drug Des.* **2008**, *4*, 250−258.

(17) Wilson, G. L.; Lill, M. A. Integrating structure-based and ligand-based approaches for computational drug design. *Future Med. Chem.* **2011**, *3*, 735−750.

(18) Holliday, J. D.; Kanoulas, E.; Malim, N.; Willett, P. Multiple search methods for similarity-based virtual screening: analysis of search overlap and precision. *J. Cheminformatics* **2011**, *3*, No. 29.

(19) Krueger, D. M.; Evers, A. Comparison of Structure- and Ligand-Based Virtual Screening Protocols Considering Hit List Complementarity and Enrichment Factors. *ChemMedChem* **2010**, *5*, 148−158.

(20) Chen, Z.; Tian, G.; Wang, Z.; Jiang, H.; Shen, J.; Zhu, W. Multiple Pharmacophore Models Combined with Molecular Docking: A Reliable Way for Efficiently Identifying Novel PDE4 Inhibitors with High Structural Diversity. *J. Chem. Inf. Model.* **2010**, *50*, 615−625.
(21) Feher, M. Consensus scoring for protein-ligand interactions. *Drug Discov. Today* **2006**, *11*, 421−428.
(22) Cross, J. B.; Thompson, D. C.; Rai, B. K.; Baber, J. C.; Fan, K. Y.; Hu, Y.; Humblet, C. Comparison of Several Molecular Docking Programs: Pose Prediction and Virtual Screening Accuracy. *J. Chem. Inf. Model.* **2009**, *49*, 1455−1474.
(23) Bergner, A.; Parel, S. P. Hit Expansion Approaches Using Multiple Similarity Methods and Virtualized Query Structures. *J. Chem. Inf. Model.* **2013**, *53*, 1057−1066.
(24) Willett, P. Combination of Similarity Rankings Using Data Fusion. *J. Chem. Inf. Model.* **2013**, *53*, 1−10.
(25) Svensson, F.; Karlen, A.; Skold, C. Virtual Screening Data Fusion Using Both Structure- and Ligand-Based Methods. *J. Chem. Inf. Model.* **2012**, *52*, 225−232.
(26) Klon, A. E.; Glick, M.; Davies, J. W. Combination of a naive Bayes classifier with consensus scoring improves enrichment of high-throughput docking results. *J. Med. Chem.* **2004**, *47*, 4356−4359.
(27) *Discovery Studio 3.1 Guide*; Accelrys Inc.: San Diego, 2012; http://www.accelrys.com.
(28) Carlson, H. A. Protein flexibility and drug design: how to hit a moving target. *Curr. Opin. Chem. Biol.* **2002**, *6*, 447−452.
(29) Meagher, K. L.; Carlson, H. A. Incorporating protein flexibility in structure-based drug discovery: Using HIV-1 protease as a test case. *J. Am. Chem. Soc.* **2004**, *126*, 13276−13281.
(30) Damm, K. L.; Carlson, H. A. Exploring experimental sources of multiple protein conformations in structure-based drug design. *J. Am. Chem. Soc.* **2007**, *129*, 8225−8235.
(31) Cozzini, P.; Kellogg, G. E.; Spyrakis, F.; Abraham, D. J.; Costantino, G.; Emerson, A.; Fanelli, F.; Gohlke, H.; Kuhn, L. A.; Morris, G. M.; Orozco, M.; Pertinhez, T. A.; Rizzi, M.; Sotriffer, C. A. Target Flexibility: An Emerging Consideration in Drug Discovery and Design. *J. Med. Chem.* **2008**, *51*, 6237−6255.
(32) B-Rao, C.; Subramanian, J.; Sharma, S. D. Managing protein flexibility in docking and its applications. *Drug Discov. Today* **2009**, *14*, 394−400.
(33) Zhou, S.; Li, Y.; Hou, T. Feasibility of using molecular docking-based virtual screening for searching dual target kinase inhibitors. *J. Chem. Inf. Model.* **2013**, *53*, 982−996.
(34) Ma, D.-L.; Chan, D. S.-H.; Leung, C.-H. Drug repositioning by structure-based virtual screening. *Chem. Soc. Rev.* **2013**, *42*, 2130−2141.
(35) Totrov, M.; Abagyan, R. Flexible ligand docking to multiple receptor conformations: a practical alternative. *Curr. Opin. Struct. Biol.* **2008**, *18*, 178−184.
(36) Rueda, M.; Bottegoni, G.; Abagyan, R. Consistent Improvement of Cross-Docking Results Using Binding Site Ensembles Generated with Elastic Network Normal Modes. *J. Chem. Inf. Model.* **2009**, *49*, 716−725.
(37) Rueda, M.; Bottegoni, G.; Abagyan, R. Recipes for the Selection of Experimental Protein Conformations for Virtual Screening. *J. Chem. Inf. Model.* **2010**, *50*, 186−193.
(38) Leung, T.; Manser, E.; Tan, L.; Lim, L. A novel serine/threonine kinase binding the Ras-related RhoA GTPase which translocates the kinase to peripheral membranes. *J. Biol. Chem.* **1995**, *270*, 29051−29054.
(39) Dong, M.; Yan, B. P.; Liao, J. K.; Lam, Y.-Y.; Yip, G.; Yu, C.-M. Rho-kinase inhibition: a novel therapeutic target for the treatment of cardiovascular diseases. *Drug Discov. Today* **2010**, *15*, 622.
(40) Liu, S.; Goldstein, R. H.; Scepansky, E. M.; Rosenblatt, M. Inhibition of rho-associated kinase signaling prevents breast cancer metastasis to human bone. *Cancer Res.* **2009**, *69*, 8742−8751.
(41) Kubo, T.; Yamaguchi, A.; Iwata, N.; Yamashita, T. The therapeutic effects of Rho-ROCK inhibitors on CNS disorders. *Ther. Clin. Risk Manag.* **2008**, *4*, 605.
(42) Mueller, B. K.; Mack, H.; Teusch, N. Rho kinase, a promising drug target for neurological disorders. *Nat Rev. Drug Discov.* **2005**, *4*, 387−398.
(43) Berman, H. M.; Westbrook, J.; Feng, Z.; Gilliland, G.; Bhat, T. N.; Weissig, H.; Shindyalov, I. N.; Bourne, P. E. The Protein Data Bank. *Nucleic Acids Res.* **2000**, *28*, 235−242.
(44) Liu, T.; Lin, Y.; Wen, X.; Jorissen, R. N.; Gilson, M. K. BindingDB: a web-accessible database of experimentally determined protein-ligand binding affinities. *Nucleic Acids Res.* **2007**, *35*, D198−D201.
(45) Rogers, D.; Brown, R. D.; Hahn, M. Using extended-connectivity fingerprints with Laplacian-modified Bayesian analysis in high-throughput screening follow-up. *J. Biomol. Screen.* **2005**, *10*, 682−686.
(46) Friesner, R. A.; Murphy, R. B.; Repasky, M. P.; Frye, L. L.; Greenwood, J. R.; Halgren, T. A.; Sanschagrin, P. C.; Mainz, D. T. Extra precision glide: Docking and scoring incorporating a model of hydrophobic enclosure for protein-ligand complexes. *J. Med. Chem.* **2006**, *49*, 6177−6196.
(47) Kaminski, G. A.; Friesner, R. A.; Tirado-Rives, J.; Jorgensen, W. L. Evaluation and reparametrization of the OPLS-AA force field for proteins via comparison with accurate quantum chemical calculations on peptides. *J. Phys. Chem. B* **2001**, *105*, 6474−6487.
(48) Sutter, J.; Li, J.; Maynard, A. J.; Goupil, A.; Luu, T.; Nadassy, K. New Features that Improve the Pharmacophore Tools from Accelrys. *Curr. Comput.-Aided Drug Des.* **2011**, *7*, 173−180.
(49) Rogers, D.; Hopfinger, A. J. Application of genetic function approximation to quantitative structure-activity-relationships and quantitative structure-property relationships. *J. Chem. Inf. Comput. Sci.* **1994**, *34*, 854−866.
(50) Chen, L.; Li, Y.; Zhao, Q.; Peng, H.; Hou, T. ADME Evaluation in Drug Discovery. 10. Predictions of P-Glycoprotein Inhibitors Using Recursive Partitioning and Naive Bayesian Classification Techniques. *Mol. Pharmaceutics* **2011**, *8*, 889−900.
(51) Tian, S.; Wang, J.; Li, Y.; Xu, X.; Hou, T. Drug-likeness Analysis of Traditional Chinese Medicines: Prediction of Drug-likeness Using Machine Learning Approaches. *Mol. Pharmaceutics* **2012**, *9*, 2875−86.
(52) Wang, S.; Li, Y.; Wang, J.; Chen, L.; Zhang, L.; Yu, H.; Hou, T. ADMET Evaluation in Drug Discovery. 12. Development of Binary Classification Models for Prediction of hERG Potassium Channel Blockage. *Mol. Pharmaceutics* **2012**, *9*, 996−1010.
(53) Hou, T.; Wang, J.; Zhang, W.; Xu, X. ADME evaluation in drug discovery. 7. Prediction of oral absorption by correlation and classification. *J. Chem. Inf. Model.* **2007**, *47*, 208−218.
(54) Shen, M.; Tian, S.; Li, Y.; Li, Q.; Xu, X.; Wang, J.; Hou, T. Drug-likeness analysis of traditional Chinese medicines: 1. property distributions of drug-like compounds, non-drug-like compounds and natural compounds from traditional Chinese medicines. *J. Cheminformatics* **2012**, *4*, 31.
(55) Qiao, X. B.; Hou, T. J.; Zhang, W.; Guo, S. L.; Xu, S. J. A 3D structure database of components from Chinese traditional medicinal herbs. *J. Chem. Inf. Comput. Sci.* **2002**, *42*, 481−489.
(56) Bemis, G. W.; Murcko, M. A. The properties of known drugs 0.1. Molecular frameworks. *J. Med. Chem.* **1996**, *39*, 2887−2893.